

Cone cracks and the Auerbach relationship in diamond

M. R. ACTON*, J. WILKS

Department of Physics, Clarendon Laboratory, University of Oxford, Parks Road, Oxford, OX1 3PU, UK

Measurements have been made of the critical load, P_c , required to produce a cone crack when a polished surface of diamond is indented by a spherically tipped diamond indenter. Particular attention was paid to the polishing of both the indenter and the flat surface in order to reduce the scatter often observed in this type of experiment. The polish on the flat was a compromise between being as fine as possible to avoid scatter but not so fine that the indenter fractured before the flat. Measurements were made with indentors of radius, R , ranging from 50 to 320 μm , and the values of P_c were found to be approximately proportional to R , the so-called Auerbach relationship. These results are discussed in terms of a recent treatment of cone cracks in isotropic brittle solids by Mougnot and Maugis. After allowing for various uncertainties introduced by the anisotropy of diamond, reasonable agreement is obtained for the absolute magnitudes of P_c . The sizes of the cone cracks are significantly larger than those predicted, possibly because the anisotropy of the diamond causes the shape of the crack to depart from that of an ideal cone.

1. Introduction

A Hertz indentation test is made by pressing a hard spherical indenter on to a flat surface of the material under test and observing the critical load, P_c , required to produce a cone crack of the general form shown in Fig. 1. The test is relatively simple, requires only a small area of material, and is widely used in the study of brittle materials. It is clear that the greater the critical load the greater the strength of the material but the relationship between load and strength is quite complex.

A spherical indenter of the same material as the specimen generates a radial tensile stress, σ , lying in the surface of the specimen with a magnitude given by a solution of the Hertz equation, see for example Johnson [1]

$$\begin{aligned} \sigma &= \frac{1}{2}(1 - 2\nu)P/\pi r^2 & r > a \\ &= 0 & r < 0 \end{aligned} \quad (1)$$

where ν is Poisson's ratio, P the load, r the radial distance from the centre of the indentation, and a the radius of the area of contact given by

$$a^3 = \frac{3}{2}(1 - \nu^2) \frac{PR}{E} \quad (2)$$

where R is the radius of the indenter and E is Young's modulus. The stress, σ , is the principle tensile stress and has its maximum value of $\frac{1}{2}(1 - 2\nu)P/\pi a^2$ at the edge of the area of contact, so one might expect the specimen to fracture when this stress reaches the ultimate tensile strength of the material. In this case it follows from Equation 2 that the critical loads obtained

with indentors of different radius should be proportional to the square of the radius of the indenter.

In practice, virtually all brittle materials fracture at much lower loads and stresses. Diamond is no exception and the critical stresses required to produce ring cracks are often an order of magnitude less than the theoretical tensile stress, see for example Field [2] and Whitlock and Ruoff [3]. In addition, it is often found in brittle materials that P_c is approximately proportional to R rather than to R^2 , this linear form of dependence being known as the Auerbach relationship. It is generally agreed that the strength falls below the theoretical value because of microscopic cracks in the surface of the specimen which have the effect of increasing the stress at their tips by a factor which is of the order $2(c/q)^{1/2}$ where c is the length of the crack perpendicular to the surface and q the radius of the tip which is of the order of the atomic spacing. Comparing the measured strength with the calculated value it appears that in diamond the surface cracks are of the order of 1 μm in length.

The above brief description implies that the criterion for producing a cone crack in a Hertz test is that the applied load must produce a tensile stress sufficient to extend the surface cracks at the perimeter of the area of contact. In fact, the position is more complex, because the initial crack never extends steadily to form the final cone crack. At first no cracking is visible, then as the load increases a fully developed cone crack is formed suddenly, extending outwards and downwards for a distance of the order of the radius of the area of contact. The tensile stress varies

*Present address: British Gas, Midlands Research Station, Solihull B91 2JW.

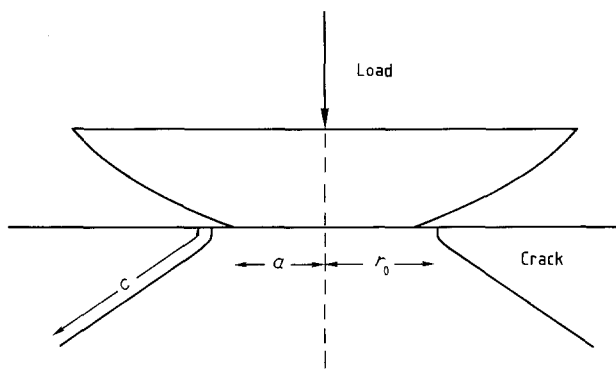


Figure 1 Schematic diagram of the production of a Hertz cone crack.

very considerably along the path of the crack and this variation must be taken into account in order to determine criteria for the production of the cracks [4].

According to Frank and Lawn [4], small cracks at the surface grow under an applied load but as they penetrate deeper below the surface, the stress field acting on them decreases rapidly. Hence, after some increase in length they eventually stop growing and do not grow again until the applied stress reaches a new critical value, large enough to cause the crack to extend suddenly and irreversibly to form the full cone. It is this final critical load which is observed in the Hertz test. According to these authors the form of the stress field in the specimen has the effect of bringing all sufficiently small cracks to a common length before the load reaches the final critical value P_c , and this effect is responsible for the Auerbach relationship $P_c \propto R$. However, although Frank and Lawn correctly emphasize the importance of the variation of the stress field along the crack, their treatment is unsatisfactory on two counts. First, they assume that the crack originates on the perimeter of the area of contact whereas the crack is generally observed to form at somewhat greater values of r [4-6], and this results in appreciable differences in the stress fields acting on the crack [7]. Secondly, the details of the calculation including the derivation of the Auerbach relationship depend very critically on the value of the Poisson's ratio. Frank and Lawn [4] took $\nu = \frac{1}{3}$ but many materials have a lower value which would cause significant differences [8]. Various modifications to the Frank and Lawn approach have been made by several authors, of which the most complete is that of Mougnot and Maugis [8] described below.

Other authors [9-12] have given different explanations of the Auerbach relationship based on a model in which the surface cracks or flaws exhibit a range of lengths, the smaller flaws being the more common. It follows from Equations 1 and 2 that indentors of larger radius produce larger areas of stress in the flat surface, so a larger indenter is more likely to encounter a longer crack, and an analysis of this situation leads to an Auerbach-type relationship. However, although the distribution of crack lengths is an important factor, these treatments also are unsatisfactory. They assume that the cracks begin on the perimeter of the area of contact, and do not consider the form of the stress field; for other criticisms see Mougnot and

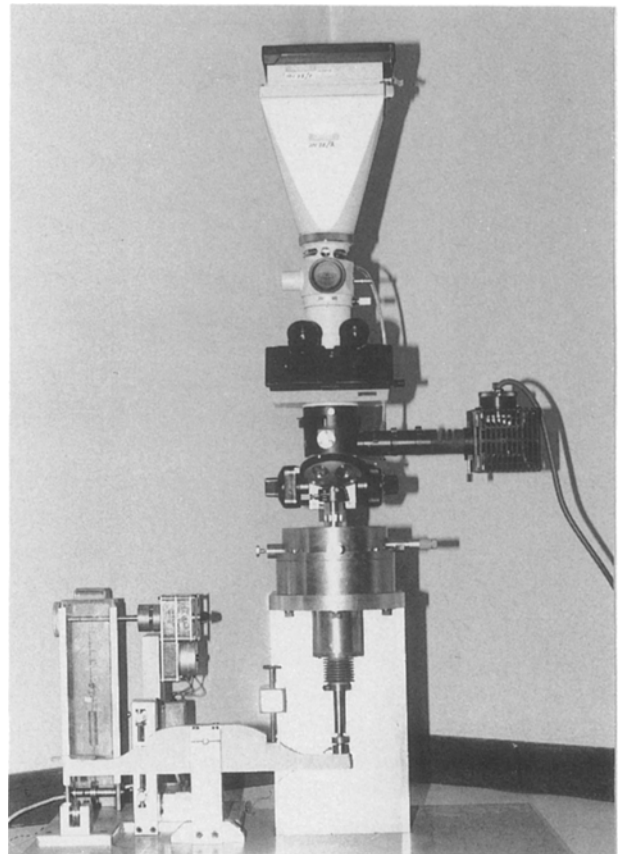


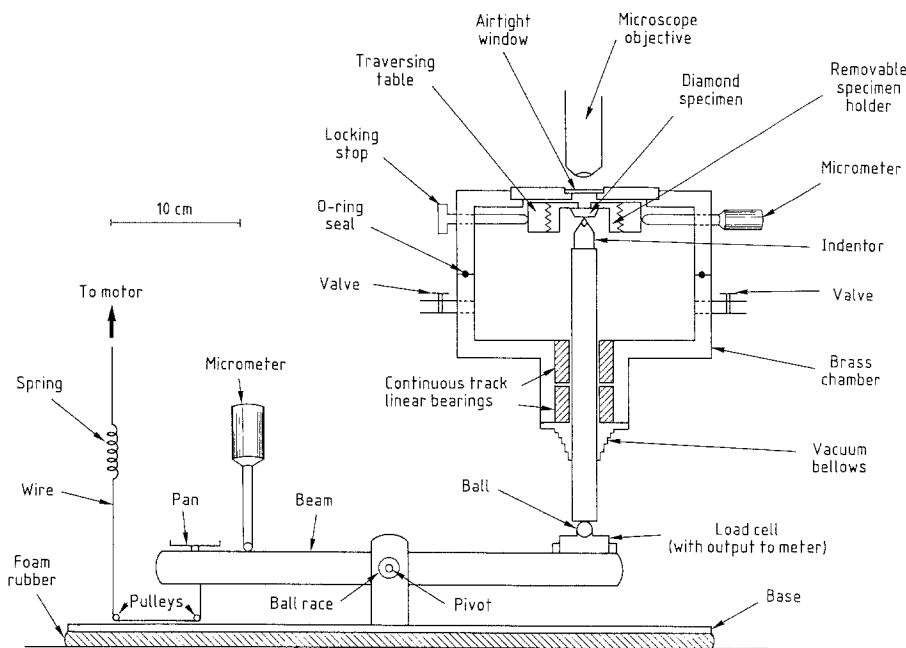
Figure 2 General view of the apparatus.

Maugis [8]. There is also the further objection that statistical treatments leading to an Auerbach relationship imply the existence of much more scatter in the values of the critical load than is often observed [13].

Diamond is a particularly good example of a brittle material showing little, if any, plastic deformation when deformed at room temperature, and therefore should be well described by theories of brittle fracture. There is, however, the complication that all the treatments mentioned above assume that the material is isotropic, whereas diamond is not, and tends to fracture along $\{111\}$ cleavage planes. Even so, a discussion by Lawn [14] suggests that the effect of this anisotropy may be relatively small. Measurements of the critical load to produce Hertz cracks in diamond have been made by Howes [15] using indentors of tungsten carbide and sapphire, and by Ikawa *et al.* [16-19] using diamond indentors. Both sets of authors used indentors of different radius, but do not discuss their results in terms of the Auerbach relationship.

The results of Ikawa *et al.* [16-19] on both natural and polished diamond faces show a great deal of scatter, for example the critical loads on polished $\{110\}$ and $\{111\}$ faces show a scatter over 10:1. Quite possibly this scatter arises because of variations in the surface of the specimens, in the roughness of the indentors, and possibly because of damage suffered by the indentors, as none of these parameters were well specified. The present experiments have been made to see whether it is possible to obtain results showing less scatter and to compare them with the predictions of the latest theoretical treatments, particularly that of Mougnot and Maugis [8].

Figure 3 Schematic diagram of the apparatus.



2. Experimental details

2.1. Apparatus

The essentials of the experimental arrangements are shown in a photograph and schematic diagram (Figs 2 and 3). The indenter is carried on the end of a stainless steel rod which runs through a pair of continuous track linear bearings in which it slides freely with virtually no play. These bearings are mounted in the base of a brass chamber which surrounds the diamonds and which permits indentations to be made in different gaseous atmospheres. The diamond flat in the form of a parallel-sided slab with polished faces is mounted as shown in Fig. 3 in a brass holder which screws into a traversing table whose position may be adjusted with micrometer screws.

The indenter is forced against the underside of the diamond by an electric motor which slowly winds in a wire which pulls down one side of a pivoted beam, the other end of which pushes up the steel rod. The force from the beam to the rod is transmitted by a steel ball to avoid any lateral thrusts and through a load cell to measure the applied force (the force on the indenter being the applied force less the weight of the rod). The spring in the length of wire (Fig. 3) is intended to smooth out any roughness or shocks arising in the motor. To ensure that the indentation is made normal to the face of the specimen, the two sides of the diamond slab are polished parallel to within $30'$, and the brass holder in the traversing table is machined so that the bearing face for the diamond is perpendicular to the axis of the steel rod.

The production of a crack is detected by viewing the lower surface of the diamond slab with a Nomarski interference microscope at a magnification of $\times 100$. The microscope was also used to inspect the tip of the indenter after each indentation to check whether any damage had occurred. This was done by unscrewing the specimen holder from the traversing table and focusing the microscope on the indenter. (With the specimen removed it was possible to use a lens with a shorter working distance and a magnification of $\times 200$).

Before making a measurement, the indenter was very slowly and gently brought against the diamond slab by driving down the left-hand end of the beam using the micrometer shown in Fig. 3, this precaution being necessary as high stresses are generated by even very moderate impacts. The indenter was slowly raised until it just made contact with the slab as shown by a black dot appearing at the centre of the point of contact. Then to make a measurement the motor was switched on and the beam steadily pulled down, the output of the load cell being fed to a chart recorder and the diamond specimen viewed in the microscope to note when the cone crack first appeared. The load on the indenter was applied at the rate of about 0.2 kg min^{-1} , and the load cell was periodically calibrated by placing weights in the pan on the left-hand end of the beam.

2.2. The diamond styli and specimens

The indenter in a Hertz test is usually much harder than the specimen, but as diamond is the hardest of all materials, the experiments have been made using diamond indentors. These diamond indentors presented two problems. First, diamonds are not isotropic and it is by no means easy to polish a smooth spherical surface. Second, because the styli are no harder than the specimen, they may fracture first. On the other hand, as both the specimen and the indenter have the same elastic constants, the indentation is not affected by frictional effects arising from relative surface motions of indenter and specimen [20].

It is difficult to produce a particular geometric surface on a diamond because the resistance of diamond to abrasion and polish depends greatly on the crystallographic orientations of the polished surface and of the direction of polish, see for example Wilks and Wilks [21]. Hence care must be taken to ensure that these differences in polishing rate do not affect the required geometric shape. Also, different directions of polish tend to give different qualities of polish, the polish generally being smoother in directions in which the diamond is polished away more rapidly. The

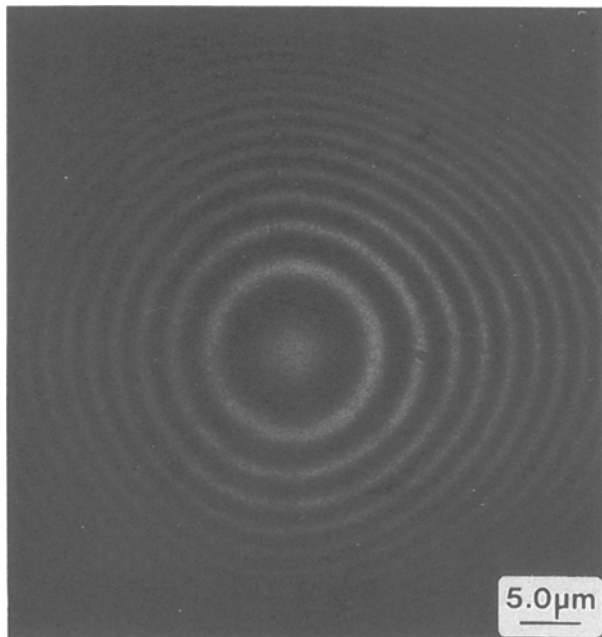


Figure 4 Newton's rings formed by an indenter of radius $115\ \mu\text{m}$.

indentors were polished in the same way as styli used in measurements of the friction [22] by swinging the diamond about horizontal and vertical axes during the polishing, the radius at the tip being determined by the distance of the wheel from the horizontal and vertical axes.

The present styli were oriented so that the tangent plane was $\{001\}$ rather than $\{110\}$ as used by Samuels and Wilks because there is some evidence that $\{001\}$ faces are more resistant than $\{110\}$ to damage by indentation [15, 16]. However, styli with $\{001\}$ tangent planes are more difficult to polish because of the greater variations in the abrasion resistance and quality of polish about a $\{001\}$ plane. Even so, by feeding the diamond slowly into the polishing wheel, surfaces were obtained which appeared smooth when viewed in the optical microscope at $\times 500$ using Nomarski technique. The geometry of the tip was determined by observing the Newton rings produced against a flat (Fig. 4). Inevitably, the styli were not quite spherical but the two principal radii differed by no more than 11% at most and generally by about 5%. Each stylus was characterized by the mean radius.

All the indentations were made on polished rather than natural diamond surfaces because the latter may contain a considerable but unknown amount of surface damage. Damage is also introduced by the polishing process, but by using controlled procedures it should be possible to obtain surfaces with reproducible characteristics. All the indentations were made on a $\langle 110 \rangle$ face polished on a good quality colourless type I diamond, this orientation being chosen as perhaps more likely to fail before the indenter. The diamond was chosen to have good octahedron faces which permitted accurate goniometry, so that the two $\{110\}$ faces forming the sides of the transparent slab could be located and oriented to within 15 min of the true $\{110\}$ plane. The faces were polished on a standard cast-iron wheel using 0 to $1\ \mu\text{m}$ diamond powder

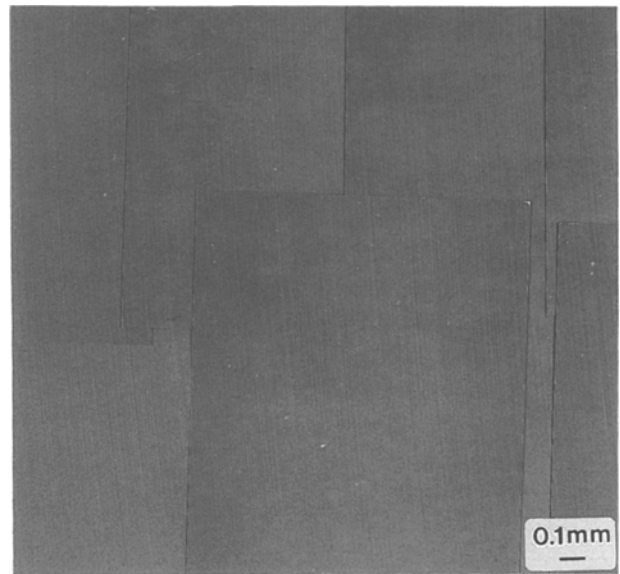


Figure 5 Optical micrograph of a $\{110\}$ diamond surface polished with 0 to $1\ \mu\text{m}$ diamond powder (Nomarski technique).

to obtain a fine finish, with the polishing lines only just visible in an optical microscope fitted with Nomarski technique (Fig. 5).

The first indentations with styli and flats prepared as above showed that the tip of the stylus suffered damage in the form of visible cracks often during the first indentation and generally after only a few indentations. An attempt was made to strengthen the stylus by a chemical etch or polish to remove surface cracks. This technique was very successful in producing a smooth surface but also produced an unwanted change in geometry in that curved facets were now visible, adjacent facets meeting with some discontinuity of curvature at their boundaries. An attempt was also made to obtain a finer polish with a wheel of dry mild steel but this wore so quickly that it was not possible to maintain the radius of the tip.

Having failed to prevent damage to the indenter by improving its polish, an attempt was made to reduce the surface strength of the specimen by polishing so as to obtain a rougher surface with deeper surface cracks. Two methods were used, polishing in the usual $\langle 001 \rangle$ direction of easy abrasion with larger 5 to $10\ \mu\text{m}$ powder, and polishing with 0 to $1\ \mu\text{m}$ powder in the hard $\langle 110 \rangle$ direction of abrasion. Both methods resulted in reduced critical loads but the use of the finer powder in the hard direction was preferred as the resulting polish was more uniform, a typical surface being shown in Fig. 6. The effect of the polish on the critical load is shown in Fig. 7 which shows the critical loads obtained in indentations on fine and coarsely polished surfaces as described above using indentors of similar but not identical radius. The lines on the figure indicate the full range of the observed values and n the number of indentations on each surface. The critical loads on the coarsely polished surface are much reduced and the styli making these indentations showed no sign of damage; therefore this type of polished surface was used for the main experiment.

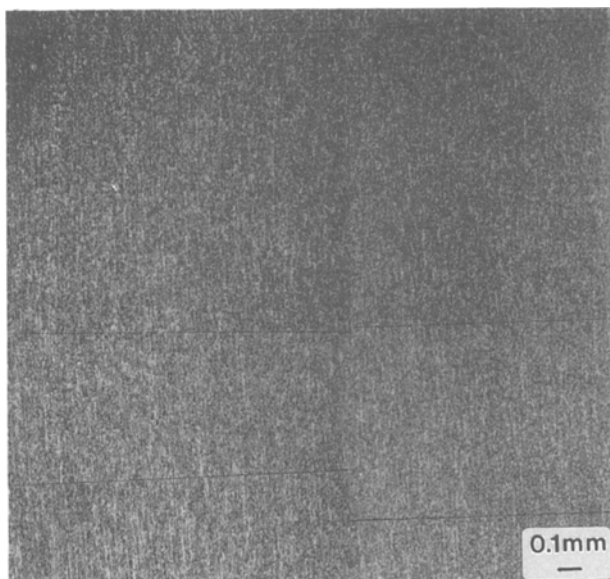


Figure 6 Optical micrograph of a {110} diamond surface polished with 0 to 1 μm powder in the hard direction (Normarski technique).

3. Results

3.1. Critical loads

The critical load P_c required to produce a conical crack was measured as a function of the radius of the indenter. The radii available were limited at the lower end by the difficulty of forming radii smaller than about 50 μm . The limit at the upper end was set by the design of the apparatus which could only accommodate loads up to about 5 kg weight.

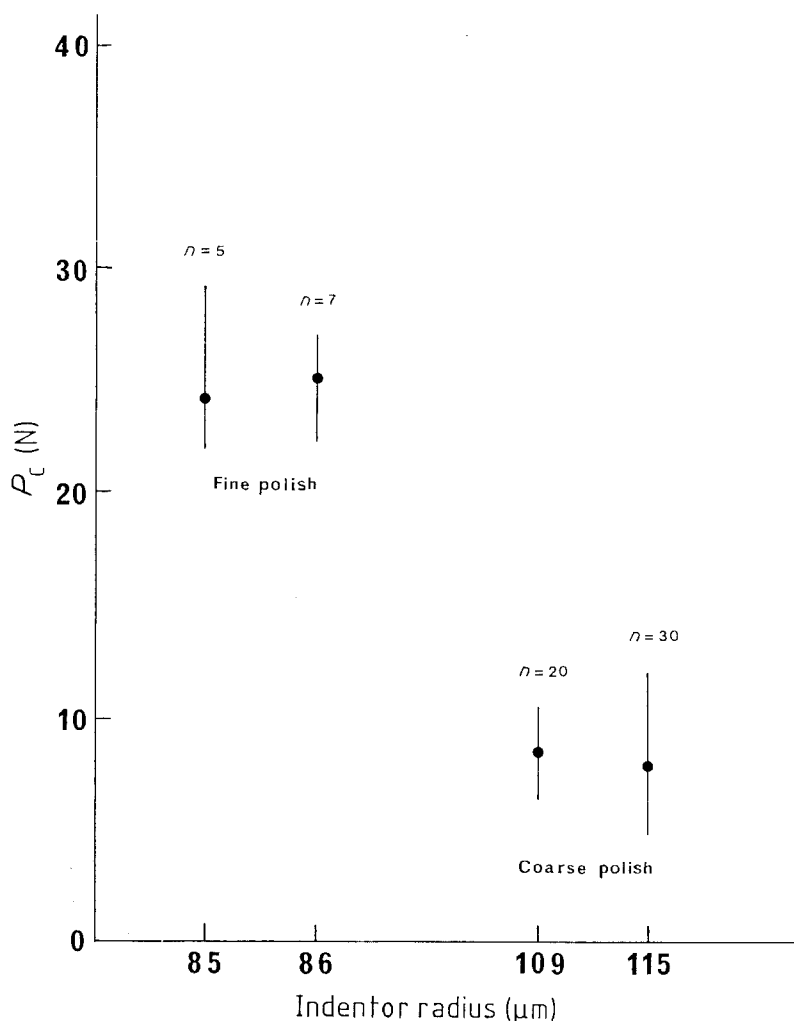


Figure 7 The critical loads required to produce cone cracks on {110} surfaces of diamond with smooth and rough polish. n is the number of indents on each specimen.

All the final measurements were made on {110} faces polished in a hard $\langle 110 \rangle$ direction using 0 to 1 μm diamond powder on a cast-iron scaife. The spacing between the indentations was at least ten times their surface radius to avoid any interference between the stress fields. When a surface was repolished, care was taken to remove all traces of previous indents.

Our results for a range of styli are shown in Fig. 8, which gives the number of indentations made with each tip, the spread of values obtained for the critical load, the mean loads, and the standard deviation for each set of values. The scatter on the critical loads is still appreciable but is considerably less than in some of the earlier work. (Most of these earlier values are presented as critical stresses rather than critical loads with the result that the scatter appears much reduced because the stresses are proportional to $P^{1/3}$.) We see that the critical load varies linearly with the radius of the indenter for the smaller radii and then rises some-what faster than linearly for the larger radii.

Experiments which give the critical load as a function of indenter radius have also been made by Ikawa *et al.* [16–19]. However, these authors present their results as the mean pressures, p_0 , on the diamond or the tensile stresses, σ_m , in the surface at the edge of the circle of contact, calculated from the loads by the Hertz relationship

$$p_0 = P/\pi\alpha^2 = (P^{1/3}/\pi) [2E/3(1 - \nu)^2 R]^{2/3}$$

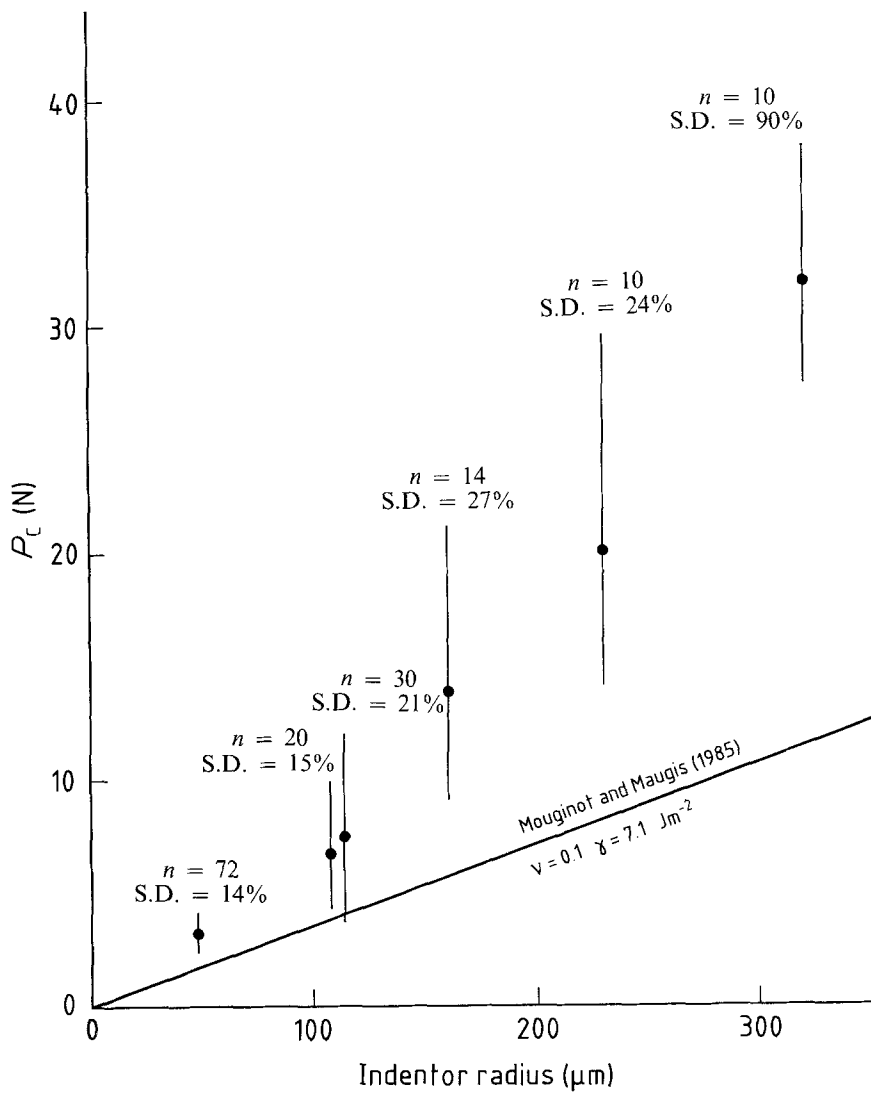


Figure 8 The critical loads required to produce cone cracks on $\{110\}$ surfaces of diamond, polished as described in the text, for a range of indentor sizes. n is the number of indents made with each indentor, and S.D. the standard deviation.

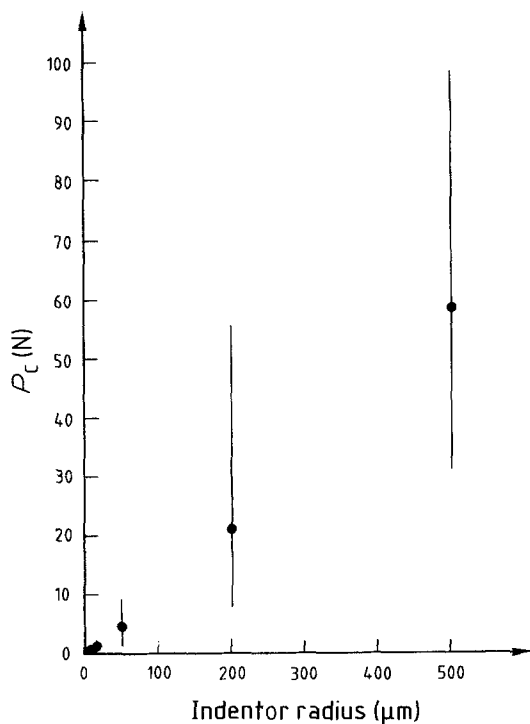


Figure 9 Loads required to produce cone cracks on natural $\{111\}$ surface of diamond, calculated from the stresses reported by Ikawa and Shimada [17].

with the appropriate values for the Young's modulus, the Poisson ratio, and the radius of the indentor. Fig. 9 shows the results of Ikawa and Shimada [17] converted back into critical loads, and we see that, although there is considerable scatter, they give a further example of the Auerbach relationship in diamond. We note that although these results were obtained on a natural $\{111\}$ surface, the critical loads are quite similar to our values obtained on polished $\{110\}$ surfaces.

3.2. Geometry of the cracks

Because diamond is crystalline and not isotropic, the cracks are not exactly circular. Fig. 10 shows a typical optical micrograph of a fine polished surface after the production of a crack. The outline of the crack tends to follow the traces of $\{111\}$ cleavage planes coming up to the surface. Two of these traces lie in $\langle 110 \rangle$ directions with the $\{111\}$ planes making angles of $35^\circ 16'$ with the surface, and four of the traces lie in $\langle 112 \rangle$ directions with the $\{111\}$ planes perpendicular to the surface. A rather similar but four-sided distortion of ring cracks is observed on $\{001\}$ surfaces, see for example [16]. In the present experiments the stylus was always oriented so that a cube axis was parallel to the $[110]$ direction on the surface.

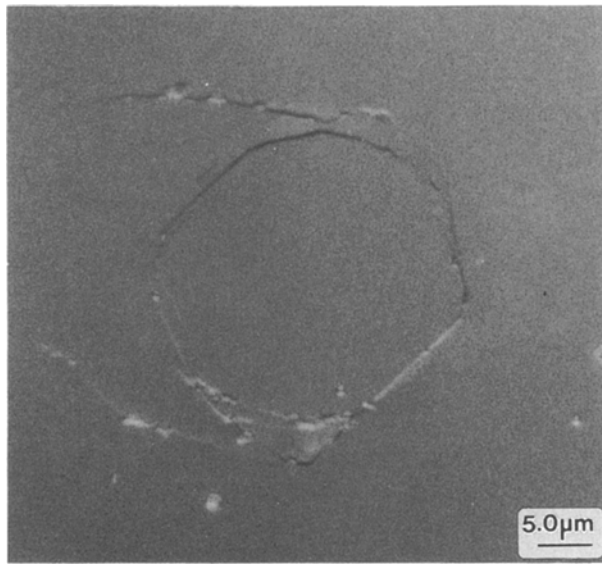


Figure 10 Ring crack on $\{110\}$ surface of diamond viewed with Normarski technique.

A characteristic feature in Fig. 10 which is seen on most cracks consists of two subsidiary cracks which run out from the approximately $\langle 110 \rangle$ sides of the main ring. It appears that these subsidiary cracks arise as the initial flaw spreads round the indenter because of a tendency for the crack to remain in the $\{111\}$ planes with $\langle 110 \rangle$ traces rather than follow the stress field. No similar branching cracks are seen at the other ends of the $\langle 110 \rangle$ sides of the ring, therefore the crack must have initiated on the right-hand side of the ring and then run round on an upper and lower path to the left, each path splitting into two as the stress field turns away from the $\langle 110 \rangle$ traces. We would expect the crack to initiate on one of the $\langle 112 \rangle$ sets of $\{111\}$ planes as these are perpendicular to the surface and experience the greater resolved tensile strength. On the other hand, when the conical crack has formed and is beginning to expand it will prefer to follow the $\langle 110 \rangle$ set of $\{111\}$ planes because these are more nearly inclined to the position of the stress field. The geometrical form of the ring cracks is readily seen on well polished surfaces, but in our main experiments with a rougher polish both the critical loads and the rings were smaller so detail was lost in the surface roughness. However, it seems likely that the geometries of the cracks were similar to those described above.

The length of the ring cracks measured down from the surface is not readily obtained by optical inspections. However, order of magnitude estimates were found by polishing down on the surface of the diamond and observing when the cracks disappeared, while at the same time measuring the depth of surface removed by monitoring the depths of three abrasion cuts with a Talysurf. It was found that the cracks were seldom uniformly deep, being generally deepest on the side where they initiated and least deep on the opposite side between the two subsidiary cracks, presumably because the elastic energy driving the crack is divided when the subsidiary cracks branch out. This difference in depth was most marked on the rougher surfaces where the lengths were difficult to measure. To summarize our results, Table I gives the mean length of the

cracks, c , measured along the downward path of the crack, derived from about 20 cracks in all. The table also gives values for the ratio c/a where a is the radius of the area of contact calculated from the load using the Hertz equations, this ratio being a useful parameter in the theoretical treatments.

4. Theory

The most complete theoretical treatment is that of Mouginit and Maugis [8] who like previous authors calculate the stress field responsible for propagating the crack as a function of the length of the crack. They assume a uniform distribution of initial flaw cracks of length c_r and show that the load required to extend the crack depends on the value of c_r , on the radius of the indenter, and on the radial distance of the crack from the centre of the indenter. The stress field below the surface of the specimen falls off more rapidly near the edge of the area of contact than further out, so for a flaw of given length, c_r , the stress at the tip may be greater if the crack is further from the area of contact. In addition, the authors make two further assumptions. They assume that the material is isotropic and that the conical crack has circular symmetry about the axis of the indenter. That is, they assume that once a flaw crack begins to grow it immediately spreads round to form a ring, and that the subsequent growth of this ring crack may be discussed without reference to the details of this initial process. However, Fig. 10 shows that this is certainly a non-trivial assumption in the case of diamond.

Mouginit and Maugis consider a circular crack running down a distance c , measured along its length and whose radius at the surface is r_0 where $r_0 \geq a$, the radius of the area of contact. The extension of this crack is determined by the strain energy release rate, G , which is the energy provided by the stress field per unit extension of the crack length. The release rate is given by

$$G = \frac{4}{\pi^3} \frac{1 - \nu^2}{E} \frac{P^2}{a^3} \Phi(c/a) \quad (3)$$

where $\Phi(c/a)$ is a function of the elastic stress field, the Poisson ratio ν , and the initial position of the crack r_0 . Fig. 11 (from [8]) shows curves of $\Phi(c/a)$ for several values of r_0/a , calculated for $\nu = 0.22$.

The condition for a crack to extend is that the stress is sufficient to provide the additional energy required to separate the new surfaces, that is

$$G = 2\gamma \quad (4)$$

where γ is the cleavage energy for each surface. This critical condition may be rewritten using Equations 2 and 3 as

$$(\Phi)_{\text{crit}} = (9\pi^3/8)(1 - \nu^2) \frac{\gamma R^2}{E} \frac{1}{a^3} \quad (5)$$

TABLE I

	$R = 48$	$R = 103$	$R = 161$
Fine polish		$c = 3.8 \mu\text{m}$	
Rough polish	$c = 2.7 \mu\text{m}$		$c = 7.7 \mu\text{m}$
Fine polish		$c/a = 2.3$	
Rough polish	$c/a = 0.46$		$c/a = 0.53$

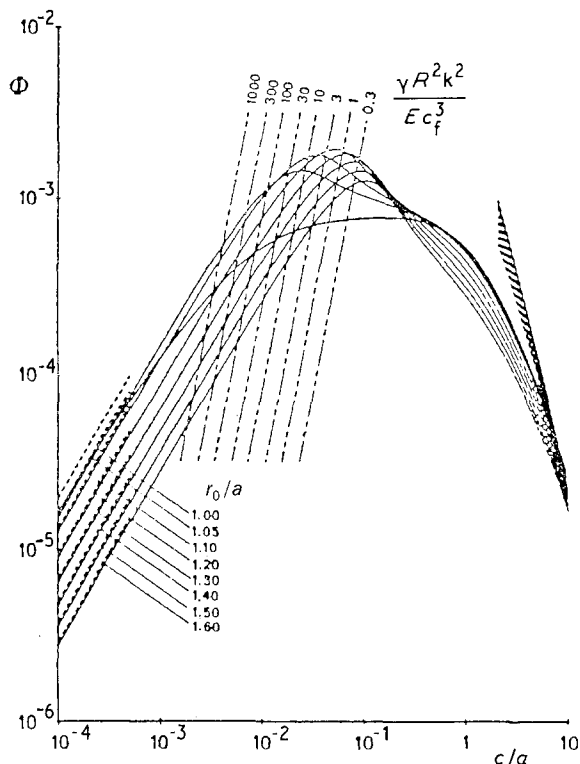


Figure 11 The function Φ plotted against c/a after Mougnot and Maugis [8], see text. The values of r_0/a run from 1.00 to 1.60.

or as $c = c_f$

$$(\Phi)_{\text{crit}} = (9\pi^3/8)(1 - \nu^2) \frac{\gamma R^2}{Ec_f^3} \left[\frac{c_f}{a} \right]^3 \quad (6)$$

Hence a plot of $\ln(\Phi)_{\text{crit}}$ against $\ln(c_f/a)$ gives a straight line of slope 3 and a set of these lines are shown in Fig. 11 for different values of the parameter $(\gamma R^2/Ec_f^3)$. A cone crack initiates when the value of G for one of the cracks reaches the value 2γ , and the corresponding value of Φ is given by the intersection of one of the straight lines and one of the curves in Fig. 11. For

example, for a flaw size c_f and $(\gamma R^2/Ec_f^3) = 10$ the critical value of Φ is where the line labelled 10 cuts the curve which gives the highest value of Φ at the intersection, in this case the curve for $r_0 = 1.10a$. Then, using Equation 2 to substitute for a^3 in Equation 3, it follows that

$$P_c = (3\pi^3/4\Phi_{\text{crit}})\gamma R \quad (7)$$

hence by taking a range of values of c_f it is possible to construct a curve of $P_c/\gamma R$ against $(R/c_f^{3/2})$ as in Fig. 12. Once the crack begins to extend, the value of (c/a) increases and both Φ and G increase so that the crack expands irreversibly until the condition $G = 2\gamma$ is again met at a greater value of (c/a) , and this second value of (c/a) gives the length of the crack formed under the critical load. These values are also shown in Fig. 12.

5. Discussion

The values for the critical load calculated by Mougnot and Maugis show at least two distinct regions (Fig. 12). First the region near the minimum in the curve of $P_c/\gamma R$ against $R/c_f^{3/2}$ which corresponds to the Auerbach regime where $P_c \propto R$. Second, the region with high values of $R/c_f^{3/2}$ corresponds to large indentors and small flaws where the stress field remains approximately constant over the length of the crack. In this second case the critical tensile stress

$$\sigma_m \propto P/a^2 \propto P^{1/3} \propto R^{2/3}$$

and the critical load $P_c \propto R^2$ as shown by the line marked "undiminishing stress field". In fact, the critical loads measured in the present experiments are proportional to the radius of the interior for the smaller radii but rise rather faster than linearly for the larger radii. Hence these results appear to correspond to that part of the curve for $P_c/\gamma R$ near and just to the right of the minimum.

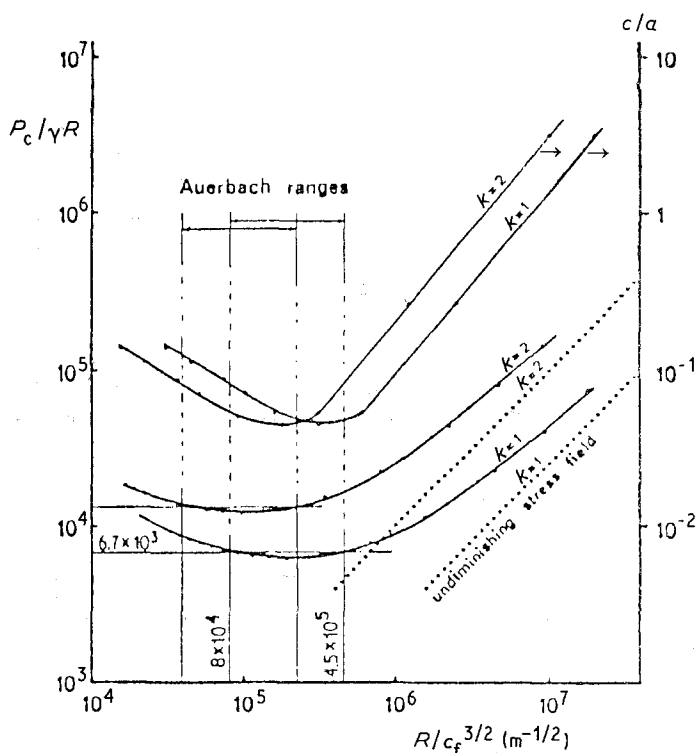


Figure 12 Critical loads, P_c (lower curves), and equilibrium lengths of crack, c (upper curves), in reduced coordinates as a function of the radius of the indenter, after Mougnot and Maugis [8], see text.

Mouginot and Maugis estimate that the value of the critical load in the Auerbach region for an isotropic solid with $\nu = 0.22$ is given by

$$P_c = 6.7 \times 10^3 K\gamma R \quad (8)$$

where $K = 2$ when the indenter and flat are of the same materials. In order to derive the value of P_c for diamond we recall that Equation 8 is derived from values of $\Phi(c/a)$ in Fig. 11 which depend on the value of the Poisson ratio, and that as diamond is not isotropic this ratio varies considerably with direction. Field [2] quotes values ranging from 0.01 to over 0.2 and suggests a mean value of 0.1, while Ruoff [23] has computed the value of 0.07 for an "isotropic polycrystalline aggregate". A complete solution of the elastic equations can only be obtained by taking account of the variation of ν along the path of the crack, but as an approximation we follow Field and take $\nu = 0.1$. Curves of $\Phi(c/a)$ given by Mouginot and Maugis for $\nu = 0.45, 0.35, 0.25, 0.22$ and 0.15 show that the influence of ν is considerable, the maximum values of $\Phi(c/a)$ for $\nu = 0.35$ and 0.15 differing by a factor of over 10. However, by a reasonable extrapolation we estimate that the maximum value of $\Phi(c/a)$ for $\nu = 0.1$ is increased from its value for $\nu = 0.22$ by a factor 2.6. We also need the appropriate value of γ for cone cracks on $\{110\}$ faces and take the value given by Field and Freeman [24] namely $\gamma = 7.1 \text{ J m}^{-2}$ (although some corrections may be needed to allow for the fact that these authors took $\nu = 0.2$). Substituting these values into Equation 8 we obtain the relationship $(P_c)_{\text{diamond}} = 3.1 \times 10^4 R$ which is shown in Fig. 8.

The theoretical line in Fig. 8 differs from the position of the measured loads by a factor of about times two. This is almost certainly as good agreement as can be expected because of the uncertainties in the calculation arising from the anisotropy of the diamond. Any discussion of the mechanics of crack propagation in anisotropic material in terms of mean values of the elastic constants can only be an approximation, and the present calculations are particularly sensitive to the value of ν . (If $\nu = 0.2$, the calculated loads are in close agreement with the observed loads for the three smallest styli, but this is of little significance in view of the various uncertainties.)

The treatment of Mouginot and Maugis also predicts the size of the cone crack produced by the critical load. Fig. 12 shows the equilibrium size, c , of the final cone crack expressed as the ratio c/a corresponding to different values of $R/c_f^{3/2}$ and $P_c/\gamma R$ for a material of Poisson ratio $\nu = 0.22$ and $\gamma/E = 5 \times 10^{-11} \text{ m}$. These results are not readily applicable to an anisotropic material with different elastic constants, but we expect the general shape of the curves for diamond to be similar though shifted to different values. The form of the curves for c/a in Fig. 12 are rather similar to those for the critical load, so c/a has a value approximately independent of $R/c_f^{3/2}$ near the Auerbach regime. In fact, Table I shows that the measured values of c/a on the rougher diamond surfaces where the critical loads followed the Auerbach relationship were approximately the same for two styli whose radii

differed by a factor of over 3. On a surface with a finer polish we would expect that c_f would be smaller so that the relevant values of $R/c_f^{3/2}$ in Fig. 12 are shifted further to the right, resulting in high values for the equilibrium crack size c/a . Table I also shows that a measured value of c/a on the smoother surface was about five times greater than that on the rougher surface.

It should be noted that the critical loads and stresses observed in a Hertz indentation experiment are so dependent on the relative values of initial crack size and indenter radius that the results of these tests cannot be expressed as a single value characterizing the strength of the diamond. The strength of diamond against fracture is much below its theoretical tensile strength and is determined by the presence of small cracks or flaws. Both our experiments and those of Ikawa and Shimada give examples of critical loads being smaller when a surface is more roughly polished. Yet in the Auerbach region the value of the critical load does not depend appreciably on the value of the initial flaw length, c_f , a result which arises from the particular geometry of the stress fields. It seems likely that this effect may account for the fact that experiments on different diamonds with different polishes and flaws sometimes give rather similar critical loads. For example, the critical stresses observed by Ikawa *et al.* [16–19] correspond to critical loads of similar magnitude to our values, even though they refer mainly to both natural and polished $\{111\}$ faces where one might expect flaws of different sizes and distributions.

Acknowledgements

We thank De Beers Industrial Diamond Division for their support of this work and for the award of a Research Studentship to M.R.A.

References

1. K. L. JOHNSON, "Contact Mechanics" (Cambridge University Press, Cambridge, 1985) p. 84.
2. J. E. FIELD, in "Science of Hard Materials", Institute of Physics Conference Series No. 75, edited by E. A. Almond, C. A. Brookes and R. Warren (Adam Hilger, Bristol, 1986) Ch. 3.
3. J. WHITLOCK and L. RUOFF, *Scripta Metall.* **15** (1981) 525.
4. F. C. FRANK and B. R. LAWN, *Proc. Roy. Soc.* **A299** (1967) 291.
5. J. S. NADEAU, *J. Amer. Ceram. Soc.* **56** (1973) 467.
6. R. WARREN, *Acta Metall.* **26** (1978) 1759.
7. T. R. WILSHAW, *J. Phys. D.* **4** (1971) 1567.
8. R. MOUGINOT and D. MAUGIS, *J. Mater. Sci.* **20** (1985) 4354.
9. I. L. OH and I. FINNIE, *J. Mech. Phys. Solids* **15** (1967) 401.
10. Y. M. TSAI and H. KOLSKY, *ibid.* **15** (1967) 29.
11. G. M. C. FISHER, *J. Appl. Phys.* **38** (1967) 1781.
12. B. HAMILTON and H. RAWSON, *J. Mech. Phys. Solids* **18** (1970) 127.
13. J. HARRISON and J. WILKS, *J. Phys. D.* **11** (1978) 73.
14. B. R. LAWN, *J. Appl. Phys.* **39** (1968) 4828.
15. V. R. HOWES, *Proc. Phys. Soc.* **74** (1959) 48.
16. N. IKAWA, S. SHIMADA and T. ONO, *Technol. Rep. Osaka Univ.* **26** (1976) 245.
17. N. IKAWA and S. SHIMADA, *ibid.* **31** (1981) 315.
18. *Idem*, *ibid.* **33** (1983) 343.
19. N. IKAWA, S. SHIMADA and T. HSUWA, *Annals CIRP* **34** (1985) 117.

20. K. L. JOHNSON, J. J. O'CONNOR and A. C. WOODWARD, *Proc. Roy. Soc.* **A334** (1973) 95.
21. E. M. WILKS and J. WILKS, *J Phys. D.* **6** (1972) 1772.
22. B. SAMUELS and J. WILKS, *J. Mater. Sci.* **23** (1988) 2846.
23. A. L. RUOFF, "High Pressure Science and Technology", Vol. 2, edited by K. D. Timmerhaus and M. S. Barber (Plenum, New York, 1979) p. 525.
24. J. E. FIELD and C. J. FREEMAN, *Phil. Mag.* **A43** (1981) 595.

*Received 13 October 1988
and accepted 16 March 1989*